Autonomous Navigation in Long-Duration, Highly Eccentric Orbits about Mars

FLORA BYARS LOWES*
NASA Manned Spacecraft Center, Houston, Texas

The problem of effective autonomous navigation for a manned spacecraft in long-duration, highly eccentric orbits is considered. A statistical error analysis using star-horizon, unknown-landmark, and surface-beacon measurements is presented for a 300-day orbital stay time about Mars. The data are processed with a Kalman filter, and the methods are evaluated for their applicability and effectiveness in minimizing estimated state errors and in producing reasonable measurement schedules. Results of the study indicate that the two optical angle-measurement methods, although constrained by the orbital geometry, can be optimally combined and used for only 4 hr during each day to produce an accuracy of less than 1 naut. mile. The estimated error in the spacecraft position obtained by continuous onboard-radar tracking of surface beacons is larger than that obtained with the optical navigation techniques. However, this result is dependent on the beacon location errors and was found to improve as knowledge of the locations increased.

Nomenclature

c	=	body center designated in Fig. 2
$E,E(t)$	=	covariance matrix of state-vector uncertainty
$H,H(t)$	=	sensitivity matrix
I,K	=	identity and weighting matrices, respectively
M	=	matrix defined by Eq. (6)
Q	=	the measurable, as defined in Eq. (1)
R	=	covariance matrix of measurement errors
$\mathbf{r},r$	=	position vector and its magnitude
r_p	=	planet radius
$S(t)$	=	transformation matrix relating orbital element perturbations to perturbations in the Cartesian position and velocity elements
$\mathbf{s}$	=	state vector (position and velocity)
t	=	time
t_0	=	arbitrary initial time
$\mathbf{u}(\ )$	=	unit vector in the direction of ( )
$\mathbf{v}$	=	velocity vector
α	=	angle defined in Fig. 2a
β	=	star-planet included angle (sextant)
θ	=	angle defined in Fig. 2b
ρ	=	range
$\dot{\rho}$	=	range-rate
ρ_0,ρ_1	=	ranges at first and second sightings (unknown landmark)
σ	=	standard deviation
$\phi(t,t_0)$	=	state transition matrix evaluated between t_0 and t

Subscripts

l	=	landmark
s	=	star
slm	=	spacecraft with respect to the beacon
vh	=	vehicle-planet horizon
vp	=	vehicle-planet center

Superscripts

T	=	transpose
-1	=	inverse
$+,-$	=	values after and before measurement

Operator

$\nabla_{\mathbf{s}}(\ )$ = gradient with respect to $\mathbf{s}$

Received August 18, 1969; presented as Paper 69-880 at the AIAA Guidance, Control, and Flight Mechanics Conference, Princeton, N.J., August 18–20, 1969; revision received January 21, 1970.

* Aerospace Engineer. Member AIAA.

Introduction

FUTURE manned interplanetary missions are likely to contain lengthy planetary stopovers; therefore, the study of the navigation problem of a manned spacecraft (SC) in a long-duration, highly eccentric orbit will become increasingly important. When considering future mission planning and anticipating more dependence on autonomous navigation in interplanetary travel, it is important to evaluate state-of-the-art navigation techniques in order to determine those techniques that are most effective and adaptable for future manned interplanetary missions. Highly eccentric orbits that must be maintained over a long period of time offer a new opportunity for navigation study because most orbital navigation analyses are documented for relatively short-duration and near-circular orbits.

A statistical error analysis using three types of orbital navigation techniques—star-horizon, unknown-landmark, and surface-beacon tracking—is presented. The basic mathematical models of these navigation techniques can be found in the referenced literature. All methods are evaluated with the assumption that the data are processed with a Kalman filter. In the mathematical model, only sensor noise is considered for the unknown-landmark navigation; however, a dynamic bias is also considered for the star-horizon and surface-beacon navigation.

The study is initiated with orbital insertion at Mars periapsis and is terminated, after a 300-day stay time, at trans-Earth injection. The initial position and velocity of the spacecraft are computed from a matched-conic interplanetary program which is coupled with a navigation and guidance analysis program.[1,2] An Earth-injection error matrix is propagated and updated during the trans-Mars phase of the mission by using a combination of onboard optical and Earth-based radar tracking. Four midcourse guidance maneuvers are implemented. The error matrices are degraded after each maneuver because of assumed correction errors. The navigation error matrix $E(t)$ resulting after orbital deboost is used initially in this study in order to present a continuous analysis with realistic errors.

The purpose of the study is to determine the capability of known autonomous navigation techniques to produce acceptable measurement schedules and to yield adequate information to minimize estimated state errors for long-duration, highly eccentric orbits.

The reference mission chosen for the study is reviewed, and the navigation system involving the three evaluated navigation measurement types is described. The analysis data are presented in two sections; 1) optical angle measurements, that is, star-horizon and unknown-landmarks, and 2) surface-beacon tracking.

Analysis

Reference Mission

The representative orbit chosen for this study is taken from a 1977 Earth-Mars conjunction-class mission involving a stay time of 300 days about Mars. The orbit (Table 1) is highly eccentric with a periapsis altitude of 200 naut miles and an apoapsis altitude of approximately 10,000 naut miles. The orbit is representative and offers opportunities for overall mission planning in the areas of maximum scientific return, minimum fuel requirements,[3] and application of navigation techniques. A schematic illustration† of the geometry of this Earth-Mars conjunction-class mission and of the orbital period about Mars is shown in Fig. 1.

Navigation System Description

Development of the navigation system equations and descriptions of the navigation methods are covered in Refs. 4–8. Principal equations are summarized in this analysis.

When the recursive navigation theory is used, measurements are made along the trajectory and are then processed by a Kalman filter to improve the state estimate. For each measurement, a sensitivity matrix $H(t)$ is computed which relates measurement deviations to state deviations. This H-matrix, expressed by

$$H(t) = \nabla_s Q \tag{1}$$

where Q is the measurable, is associated with each type of navigation measurement. As a result of each measurement and thus of the calculation of the matrix $H(t)$, the covariance matrix $E(t)$ of state uncertainties is updated and then propagated along the trajectory by the equation

$$E(t) = \phi(t,t_0)E(t_0)\phi^T(t,t_0) \tag{2}$$

where $\phi(t,t_0)$ is the state transition matrix evaluated between t_0 and t.

To avoid numerical difficulties in the update of the covariance matrix E, the standard form of the filter update equations given by

$$E^+ = (I - KH)E^- \tag{3}$$

can be written in the form[9]

$$E^+ = (I - KH)E^-(I - KH)^T + KRK^T \tag{4}$$

Table 1 Characteristics of Mars stopover orbit, 1977 Mars mission

Orbit stay time, days	300
Periapsis altitude, naut miles	200
Apoapsis altitude, naut miles	9,621.67
Inclination, deg	18.65
Eccentricity	0.697
Period, hr	11.78
Periapsis velocity in (hyperbola), fps	17,800
Periapsis velocity (ellipse), fps	14,403
Apoapsis velocity (ellipse), fps	2,568
Periapsis velocity out (hyperbola), fps	18,395

† Figure from study by J. R. Thibodeau III.

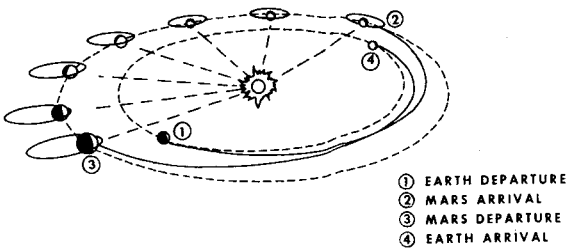

Fig. 1 Heliocentric schematic illustrating the conjunction-class mission and the parking orbit about Mars.

where

$$K = E^-H^TM^{-1} \tag{5}$$

and

$$M = HE^-H^T + R \tag{6}$$

The matrix R in Eq. (6) is the covariance matrix of the errors obtained in making the particular measurement.

For the three navigation observation types used in this study, the sensitivity matrix H can be written as follows.

1) For the star-horizon included-angle measurement, H is expressed as a 6×1 matrix defined by

$$H^T = \left[\frac{\mathbf{u}_s - (\mathbf{u}_s \cdot \mathbf{u}_{vp})\mathbf{u}_{vp}}{r_{vp}\sin\beta} \quad -\frac{\mathbf{u}_{vp}\tan\alpha}{r_{vp}} \;\vdots\; 0\right] \tag{7}$$

where $\mathbf{u}_s$ and $\mathbf{u}_{vp}$ are the unit vectors from the spacecraft to the star and to the planet, respectively. The magnitude r_{vp} and the angle β are defined by Fig. 2a, which shows the geometry of the star-horizon measurement.

2) For the unknown-landmark navigation measurement, H is again expressed as a 6×1 matrix[4] defined by

$$H^T = [0 \;\vdots\; \mathbf{u}_{\rho_0} \times \mathbf{u}_{\rho_1}] \tag{8}$$

where $\mathbf{u}_{\rho_0}$ and $\mathbf{u}_{\rho_1}$ are the unit vectors from the spacecraft to the landmark at the first and second measurement times,

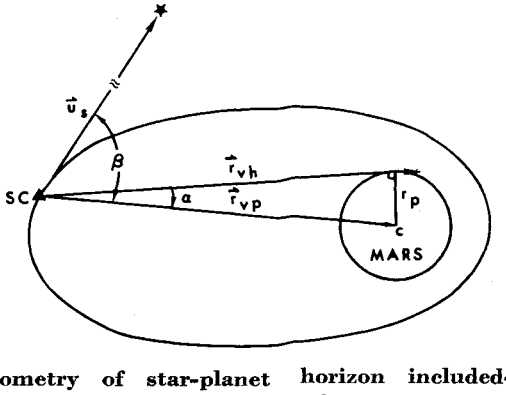

a) Geometry of star-planet horizon included-angle measurement

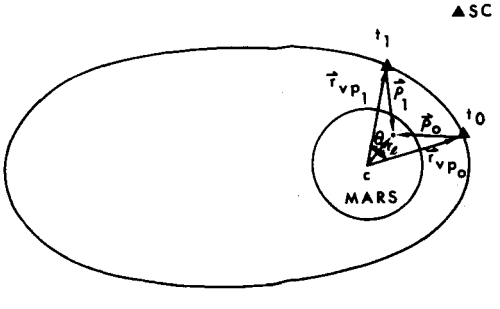

b) Geometry of unknown-landmark measurement

Fig. 2 Geometry of optical measurements used in orbital navigation.

Table 2 Nominal rms error values in navigation system, 1σ

State position uncertainty, naut miles	15
State velocity uncertainty, fps	61
Onboard sextant accuracy, arc sec	10
Optical error for unknown-landmark sightings, arc min	1
Onboard-radar accuracy:	
Range	
Noise, ft	150
Bias, ft	15
Range-rate	
Noise, fps	0.6
Bias, fps	0.03
Radius uncertainty/planet radius	0.005

respectively. The geometry of this measurement is shown in Fig. 2b.

3) For the measurement using beacons on the surface of the planet, the measurables are range ρ and range-rate $\dot{\rho}$ of the spacecraft with respect to the beacon. Thus, the matrix H is of 6×2 dimensions and is expressed by

$$H^T = \left[\begin{array}{c:c} \mathbf{u}_\rho & 0 \\ \hdashline (I - \mathbf{u}_\rho \mathbf{u}_\rho^T)\frac{\mathbf{v}_{slm}}{|\rho|} & \mathbf{u}_\rho \end{array}\right] \tag{9}$$

where $\mathbf{u}_\rho$ is the unit vector for the slant range measured from the spacecraft to the beacon, $\mathbf{v}_{slm}$ is the velocity vector of the spacecraft with respect to the beacon, and $|\rho|$ is the range magnitude. If either of the two measurements—range or range-rate—is measured separately, the matrix in Eq. (9) reduces to the 6×1 dimensions and is composed of the respective row pertaining to the measurement processed.

These matrices can be augmented[8] to include, when needed, the errors with respect to components other than position and velocity, for example, the estimation of beacon location errors.

Root mean square (rms) position and velocity errors are computed directly from the covariance matrix of navigation errors $E(t)$. However, in presenting errors in the orbital element estimation, a transformation is involved. This transformation is defined by

$$E'(t) = S(t)E(t)S^T(t) \tag{10}$$

where S is the transformation matrix relating perturbations in the orbital elements to perturbations in the Cartesian position and velocity components.

The assumed errors used for the navigation system are given in Table 2. The choice of these nominal rms errors was based on state-of-the-art knowledge.

Results and Discussion

Optical Angle Measurements

The choice of the two optical measurements—star-horizon and unknown landmarks—for evaluation in this study was based on the assumption that either method could easily be applied to the mission considered. Both methods, which are relatively well known, are easily implemented, since only an optical device (such as the sextant), the planet, a star catalog, and one man to make the measurements are needed. For a manned mission which orbits about Mars, the application of these two navigation methods is dependent upon the restrictions imposed by the orbit. Difficulties imposed by the highly eccentric orbit are the flatness of the trajectory and the extremities of the distances from the planet (near at periapsis and far at apoapsis). Other restrictions imposed by the orbit are caused by the orbital period of approximately 12 hr and by the surface lighting conditions. At all times, the orbit maintains its periapsis position in sunlight; thus, only within approximately $\pm 90°$ of periapsis is the surface in sunlight.

The star-horizon included-angle measurement is not restricted by surface lighting conditions. As long as the rim of the planet is visible and a recognizable star can be distinguished from the spacecraft, this measurement can be implemented. For the measurements in this study, the stars are chosen randomly from a computer star catalog, and the planet rim used is always that of Mars.

It was found that the star-horizon measurement was used most effectively during the outer sections of the orbit, that is, not in the proximity of periapsis, because of the relatively short time phase of the orbit near periapsis and because of the low periapsis altitude which causes a number of the stars in the star catalog to be occulted by Mars. Conversely, the outer portions of the orbit offer a free field for the star-horizon measurement because of the distance and because of the majority of the orbital time spent there. The geometry of the star-horizon measurement in Fig. 2a and the orbital characteristics in Table 1 provide a better understanding of the restrictions, measurements, and resultant data.

Figure 3a, the rms position uncertainty is plotted against the total time in orbit. For this plot, star-horizon measurements were made at 1-hr intervals for the entire orbital stay time. This schedule if unrealistic if a man is assumed to be taking measurements for 300 days; however, the use of an automatic horizon scanner is possible. Thus, Fig. 3a is presented to illustrate this measurement and the level to which it reduces the estimated position uncertainties. Because of the magnitude of the time scale, the plot produced represents an error envelope in which the upper and lower boundaries are distinguishable. The mean error produced is approximately 2.0 naut miles. The star-horizon measurement must be made often throughout the orbit in order to reduce the position uncertainties and keep them at a low level.

The only lighted part of the Mars surface lies within a 90° proximity of the periapsis line. Thus, when unknown-landmark navigation is considered, the measurements must be limited to a period of approximately 2 hr in the orbit when the spacecraft is near periapsis so that the surface features can be distinguished. Figure 3b shows the rms position uncertainties as a function of the total orbit time for unknown-landmark measurements only. These measurements were implemented during each orbit when surface landmarks were visible. One set of measurements was made every 10–15 min. From Fig. 3b, it is evident that this measurement type is effective in reducing position uncertainties and provides an approximate mean error of 1 naut mile.

In evaluating the data obtained by means of the two optical measurements, it was found that a combination of the two techniques is more effective in reducing measurement errors than either technique implemented alone. Each technique compensates for weaknesses in the other technique. These weaknesses are caused by the high eccentricity of the orbit and surface lighting conditions. Combining the two measurement types produces the plotted data in Fig. 3c. For the plot of rms position uncertainties, star-horizon measurements were made at 15-min intervals during the phase of the orbit between 160° and 195° true anomaly, and unknown-landmark measurements were made at a rate of one set every 15 min between 270° and 90° true anomaly. The measurements were made during every other orbit. Use of a combination of the two measurement types (Fig. 3c) for approximately 4 hr of navigation a day—2 hr in the vicinity of apoapsis and 2 hr in the vicinity of periapsis—is sufficient measurement to maintain an accuracy of approximately $\frac{1}{2}$ naut mile for the orbital stay time. The combination of measurements produces acceptable accuracies and provides a reasonable working schedule for the astronaut by lowering the workload required for navigation measurements. The

rms uncertainties in the orbital elements for the previously discussed combined measurement schedule are shown in Fig. 4. The errors are plotted for the first 10–12 days. This time length seems to be sufficient to analyze the effects in the orbital elements. Inspection of total position uncertainty plots indicates that once the errors are reduced sufficiently, they are decreased very little during the rest of the orbital stay time and are maintained at the decreased level by optimal scheduling of the navigation measurements. Inspection of the plotted curves in Fig. 4 indicates that the trends of the curves are established in 10 days. The rms uncertainty in the semimajor axis is shown in Fig. 4a. The error is large at the beginning of the mission, but is decreased significantly to a small uncertainty after 6 days of navigation measurements. The orbital element uncertainty curves for eccentricity and inclination are plotted in Figs. 4b and 4c, respectively. The uncertainties of the three remaining orbital elements—true anomaly, ascending node, and argument of periapsis—are presented as three respective curves in Fig. 4d. These curves follow the same trend as the curve for total position error and semimajor axis error, although these curves represent smaller values. The uncertainty values for inclination are affected the most of any of the elements by the geometry of the orbit in that the curve is, of course, oscillatory; however, the general slope follows the decreasing trend of the other plots with the boundaries of the oscillation being reduced to values of near insignificance.

Surface-Beacon Tracking

Unmanned, soft-landing probes[10] may be deployed from the orbiting manned spacecraft to study the Mars atmosphere and to collect scientific data. The probes could carry a transponder (beacon) for radar tracking by the orbiting spacecraft. Carrying the transponder might become the primary purpose of the probes. The beacons could provide almost continuous automatic tracking capability and would not be hampered by surface lighting conditions. In the study of beacon tracking, information is needed concerning the number of transponders required on the surface, the location and time of deployment, and the accuracy to which the locations must be known for sufficient orbital navigation about Mars.

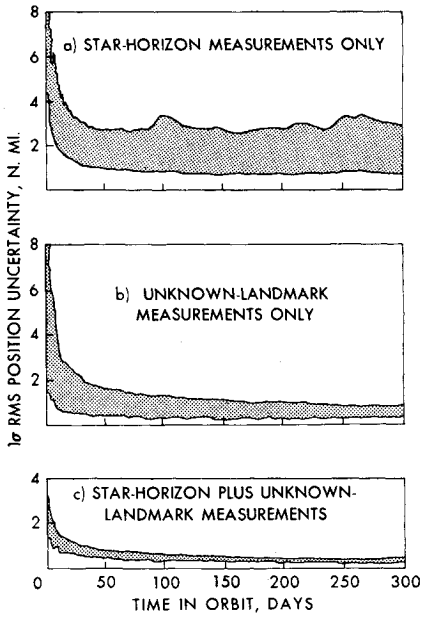

Fig. 3 Root-mean-square position uncertainties for optical navigation methods.

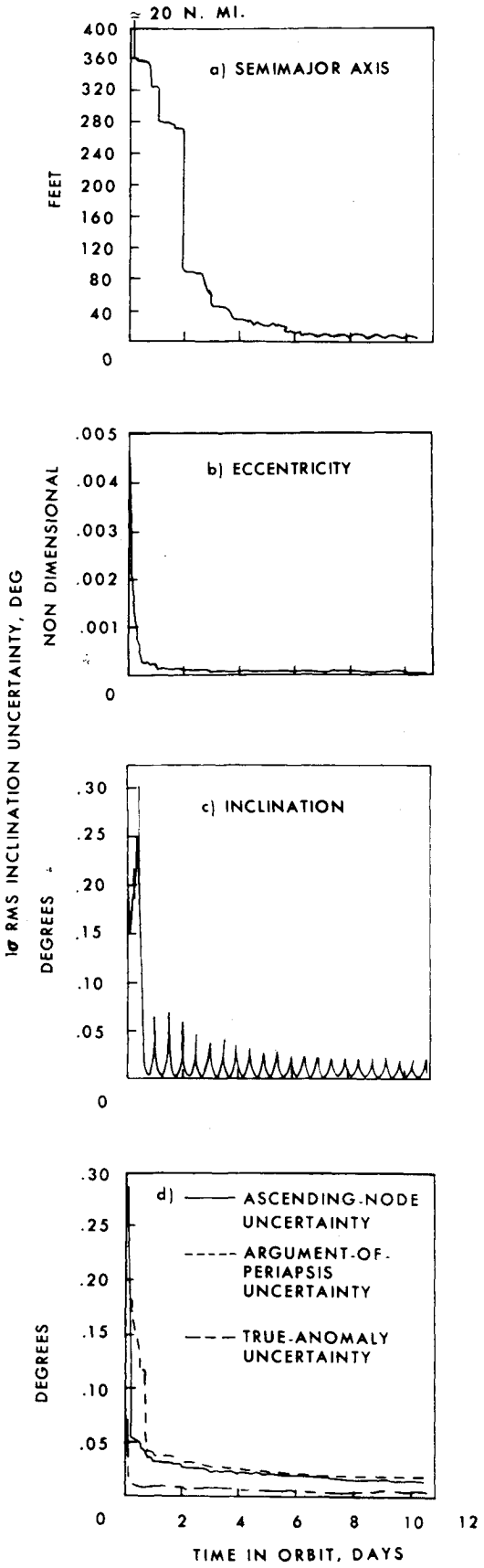

Fig. 4 Root-mean-square uncertainty for orbital elements using the combinations of star-horizon and unknown-landmark measurements.

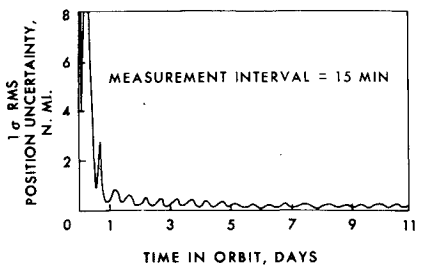

Fig. 5 Root-mean-square position accuracy for surface-beacon tracking assuming no beacon location errors (range-rate tracking only).

The deployment of some of the beacons from the spacecraft may be accomplished during the trans-Mars portion of the mission and would depend upon the fuel budget allowed for the beacons. Targeting the beacons for either the northern or southern hemisphere of Mars would cost the same if the beacons were deployed far enough away from Mars.[10] Some of the beacons would be deployed after the spacecraft had been in orbit for a period of time. Beacon deployment involves thorough, separate consideration and is not covered in depth in this study.

The study of onboard surface-beacon tracking was initiated with 10 beacons placed at longitudes 36° apart. Since the orbital plane is in the northern part of Mars for approximately 10 hr of the 12-hr orbital period, six of the beacons were placed in the northern hemisphere and four were placed in the southern hemisphere. Later, the number of beacons was decreased to four. Two beacons were spaced approximately 90° apart in each hemisphere. When spacing the beacons on the surface for continuous tracking capability, it must be remembered that because of the near-12-hr period of the orbit and the 24-hr rotational period of Mars, two orbits are required before all the planet is in view of the spacecraft. In the simulation, line-of-sight radar visibility is assumed, regardless of the distance from the spacecraft to the surface beacon, except when the beacon is below the horizon.

A comparative study of the range-rate only and range/range-rate tracking using the beacons was made with sensor noise and beacon location errors included. For the conditions implemented, the addition of the range measurements to the range-rate tracking contributed little significant data in decreasing the error values computed. Therefore, the presented data and discussion are for range-rate tracking only.

The spacecraft rms position uncertainty is plotted as a function of time in Fig. 5 for range-rate tracking using 10 surface beacons. Measurements were made at 15-min intervals, and no location errors were assumed in the beacon locations. The spacecraft position error is reduced quickly and remains approximately $\frac{1}{4}$ naut mile. Although the data are plotted for only 11 days, the curve is expected to continue at this low error value. However, this uncertainty curve is optimistic since it results from an assumption of no beacon location errors.

To determine the effect of beacon location errors on the estimation of the state of the spacecraft, a 4-mile error in the longitude and latitude and a 6000-ft error in the altitude of the beacon locations were assumed. The errors in the latitude and longitude were treated both deterministically as a bias and as a nondeterministic error source to be solved for in the filter. The altitude error was treated as a deterministic error only.

The rms position uncertainty data for range-rate measurements each 15 min using 10 surface beacons with the previously mentioned location errors are shown in Fig. 6a. This uncertainty curve is the case in which the beacon latitude and longitude errors are estimated by using the filter. In Fig. 6a, the estimated spacecraft position uncertainty is shown to be oscillatory with the orbital period and, after 1 day of tracking, lies between the bounds of approximately $1\frac{1}{2}$ to 8 naut miles. The time scale on the figure is broken so that the error obtained during the first 10 days of the orbital stay time may be compared to the error obtained 100 days later. Once the error is reduced, it tends to continue at the reduced level with continued tracking.

The estimated beacon location errors may be expected to continue to decrease and, in turn, to reduce the spacecraft position uncertainty throughout the tracking period. However, this situation does not exist with the errors assumed because the estimated beacon location errors behave in the same manner as the estimated spacecraft state uncertainties. That is, the estimated beacon location errors are reduced during the first few orbits to a level at which they tend to remain. In this case, it was found that the latitude error was reduced to approximately $\frac{1}{4}$ naut miles, but that the longitude error was reduced only to approximately $1\frac{1}{2}$ naut miles thus maintaining sizable errors in the surface beacon locations.

The plotted data for the study in which the location errors are treated deterministically (i.e., the beacon location errors are not estimated) are not presented because these data produced the same effects as those in Fig. 6 (with the exception of raising the error envelope approximately $\frac{3}{4}$ naut mile).

In comparing the curve in Fig. 6a to that in Fig. 5, it is evident that errors in surface-beacon locations have a marked effect in raising the limits of the rms position error curves. In examining the individual components of position error (i.e., altitude, range, and track), it was found that the altitude uncertainty is reduced very early to a small error value, even when the beacons are assumed to have large location errors. The track uncertainty tends to decrease slowly, and the downrange error, which maps into a timing error, remains as the largest component of the total estimated position uncertainty.

The possibility of increasing the amount of tracking during the early portions of the orbital mission was investigated with the objective of reducing the estimated errors in the beacon locations and thus reducing the spacecraft position

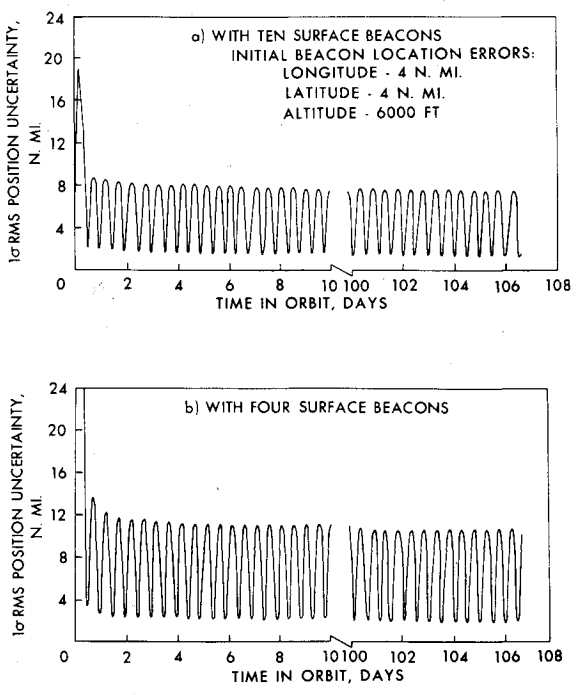

Fig. 6 Root-mean-square position accuracy for range-rate tracking using ten (a) and four (b) surface beacons (location errors estimated), respectively. a) With 10 surface beacons. b) With four beacons.

uncertainty. However, the increase was found to have little effect.

A simultaneous study using only four surface beacons was implemented. In part b of Fig. 6, the rms position uncertainty of the spacecraft is plotted as a function of time in orbit for the same conditions and in the same manner as the data in Fig. 6a, except that only four beacons were used. The use of the four beacons—as opposed to the use of 10 beacons—raises the upper boundary of the estimated position error envelope approximately 4 naut miles and the lower boundary approximately $\frac{1}{2}$ naut miles. In further study, it was found that if the locations of these four beacons were assumed to be better known, the boundaries of the error curve fall within the limits of the error curve for the ten beacons, as plotted in Fig. 6a. The data tend to indicate that fewer beacons can be used if the ability to determine their locations is improved. A minimum of four surface beacons properly spaced for use in all orbits could provide enough information to the spacecraft for orbit maintenance, depending again on the knowledge of the beacon locations.

The uncertainties in the spacecraft orbital elements using surface-beacon tracking are not plotted. The only element that showed any detectable error was the semimajor axis, which maintained an oscillatory uncertainty bounding between $\sim$100 and 450 ft. The error in the estimations of the other five orbital elements was reduced immediately to an insignificant level.

Concluding Remarks

Regarding future mission planning, it is important to determine the effectiveness of some of the known autonomous navigation methods, as well as their adaptiveness to such missions. A statistical error analysis using star-horizon included-angle measurements, unknown-landmarks, and surface beacons for navigation in a long-duration, highly eccentric orbit about Mars has been presented. It was found that these methods could be directly applied to such an orbit with only slight modifications, but that the geometrical orbital restrictions must be considered in the optimal scheduling of navigation measurements.

When used in combination for 4 hr a day, the onboard optical measurements—unknown-landmark and star-horizon—were found to produce an accuracy of less than 1 naut mile for the 300-day orbital stay time. It was found that the use of these measurements in an optimal manner for the reduction of the astronaut workload did not degrade this accuracy.

In contrast, surface-beacons tracking from the spacecraft does not reduce the estimated state errors as well as optical measurements do if fairly large beacon location errors are assumed. However, surface-beacon tracking offers the advantage of almost continuous automatic tracking and is not hampered by lighting restrictions. For surface-beacon-tracking measurements to be comparable in value to the optical measurements, an accurate technique for determining the beacon locations on the surface is required.

References

[1] Bond, V. R., "Matched-Conic Solutions to Round-Trip Interplanetary Trajectory Problems that Insure State-Vector Continuity at all Boundaries," TN D-4942, Jan. 1969, NASA.

[2] Lowes, F. B. and Murtagh, T. B., "Navigation and Guidance Systems Performance for Three Typical Manned Interplanetary Missions," TN D-4629, July 1968, NASA.

[3] Taylor, J. J. and Wilson, S. W., Jr., "A Minimum-Energy Mission for the Manned Exploration of Mars," TN D-5502, July 1969, NASA.

[4] Levine, G. M., "A Method of Orbital Navigation Using Optical Sightings to Unknown Landmarks," *AIAA Journal*, Vol. 4, No. 11, Nov. 1966, pp. 1928–1931.

[5] Marscher, W., "A Unified Method of Generating Conic Solutions," Rept. R-479, Feb. 1965, MIT Instrumentation Lab., Massachusetts Institute of Technology, Cambridge, Mass.

[6] Murtagh, T. B., Lowes, F. B., and Bond, V. R., "Navigation and Guidance Analysis of a Mars Probe Launched from a Manned Flyby Spacecraft," TN D-4512, April 1968, NASA.

[7] Battin, R. H., *Astronautical Guidance*, McGraw-Hill, New York, 1964.

[8] *User's Manual for Mark II Error Propagation Program*, Philco WDL-TR 2758, Feb. 1966, Philco Corp., Western Development Labs., Palo Alto, Calif.

[9] Bryson, A. E. and Ho, Y.-C., *Applied Optimal Control*, Blaisdell, New York, 1969.

[10] Murtagh, T. B., "Planetary Probe Guidance Accuracy Influence Factors for Conjunction Class Missions," TN D-4852, Jan. 1969, NASA.